

Exact self-similar shapes in viscous fingering

Martine Ben Amar

Laboratoire de Physique Statistique, Ecole Normale Supérieure, 24 rue Lhomond, 75231 Paris CEDEX 05, France

(Received 2 November 1990)

Analytical self-similar profiles of the Saffman-Taylor experiment in a sector of a disk are determined by conformal mapping in the absence of surface tension. I show the existence of a continuous set of symmetric solutions in either the convergent or divergent fluid-flow case.

This paper gives the self-similar shapes of viscous fingers in an arbitrary open sector cell in the absence of surface tension. Up to now, analytical solutions have been discovered for only two typical geometries of the Hele-Shaw cells: the classical linear¹ one corresponding to $\theta_0=0$ and the divergent right-angle² one ($\theta_0=\pi/2$). First introduced experimentally,² the sector geometry, intermediate between the linear and the circular geometry, is a very useful tool for understanding the spatial and time evolution of systems in situations far from equilibrium, like seeds in an undercooled melt. Unfortunately, the lack of known exact analytical results has inhibited the complete understanding of this growth process.

I propose here a systematic way to derive these symmetric profiles (without any guessing) corresponding to either divergent or convergent flow. I generalize the method of McLean and Saffman³ to any geometry and find a continuous set of solutions for an arbitrary angle between $-2\pi < \theta_0 < \pi$. The experiment² indicates that only one solution is selected among this continuum which is characterized by the dimensionless width λ of the finger. In the divergent case, the self-similar shape looks like a petal, and λ is the ratio between the petal angle measured at the center and the cell angle. For the convergent flow, λ is the ratio between the angle of the finger tails and the sector. As for other instabilities,⁴ we expect that the neglected surface tension, once introduced, will select the self-similar pattern, and thus λ . In any case, the knowledge of exact results is a first step to explain the selection mechanism which occurs for this instability; any tentative treatment will be mostly perturbative, even if it is in some singular sense like the WKB method.⁵ This is the reason why it previously had been applied to only the right-angle sector.⁶ Moreover, once selected, these analytical solutions reproduce the experimental fingers at low surface tension.

Since the pioneering work of Saffman and Taylor,¹ the viscous fingering in a Hele-Shaw cell has induced numerous experimental,⁷ numerical,^{3,8} and analytical^{1,3,9,10} studies (for a review, see Refs. 4, 7, and 9). This instability has always been a prototype to understand the evolution of growing patterns. Similar to the solidification process at low growth rate, but in many respects much simpler, it has aided in the understanding of the rather sophisticated role of a tiny surface-tension amount, whether it is isotropic¹⁰ or not,¹¹ the effects of local perturbations,¹² the stability of steady-state solutions,¹³ etc. Fundamental but open questions, such as the effect of capil-

larity on the time-dependent pattern¹⁴ or the link between the diffusion-limited aggregation model and macroscopic continuous models,² have been answered in part. Nevertheless, many of these results concern the linear geometry and not the circular one which is much more common in nature. Either the viscous pattern in the Paterson¹⁵ geometry or the growing seeds show very regular petals, self similar in times, localized in fictitious sectors. This is true, at least in the first stage of growth. Due to this similarity with the Saffman and Taylor finger (called hereafter ST), Paterson has tried a conformal transformation of the ST solutions to interpret his experiment. Although unsuccessful, this was the first attempt to relate known established results of the linear channel to the unknown circular geometry. This analytical family of solutions shows that the sector geometry presents continuous features which can be extrapolated to interpret dynamical processes in the absence of rigid walls.

Let us recall here that viscous fingering is a free-boundary problem. The fluid flow of the pushed oil is Laplacian, since $\mathbf{v}=\nabla\phi$ and $\Delta\phi=0$ if one assumes the Darcy law for the Hele-Shaw cell. In the absence of surface tension, the interface is an equipotential of ϕ and satisfies the continuity equation: $\mathbf{n}\cdot\nabla\Phi=\mathbf{n}\cdot d\mathbf{r}_{\text{int}}(t)/dt$, with $\mathbf{r}_{\text{int}}(t)$ a current point of the interface and \mathbf{n} the normal at this point. Assuming self-similarity is a convenient simplification of time-dependent free-boundary problems, but very often not rigorous. Hakim² has shown that self-similar solutions form an exact class of solutions if one neglects surface tension and assumes that the experiment is done with a constant extraction or injection rate imposed at infinity. For these self-similar solutions, observed in the experiment, the interface evolves in time as $(2t+1)^{1/2}$ for divergent flow or $(1-2t)^{1/2}$ for convergent flow (in this case, time grows from negative values). Perhaps the comparison between self-similar solutions and steady-state fingers displaced in a channel does not seem obvious. In order to emphasize the link between these two instabilities, a proposal¹⁶ to transform the sector geometry (π_1 plane) into an infinite strip (π plane) by conformal mapping is as follows: $z=(2/\theta_0)\ln(z_1)$ with θ_0 positive when air pushes oil from the center, ($0\leq\theta_0<2\pi$), and negative when from the periphery, ($-2\pi<\theta_0\leq 0$). Figures 1-3 show the corresponding characteristic points of the two planes. This mapping transforms the petal shape of the interface, for a divergent channel, (Fig. 1, π_1 plane) into a more familiar finger shape (Fig. 3, π plane), while the walls become parallel. Note that the origin of the sec-

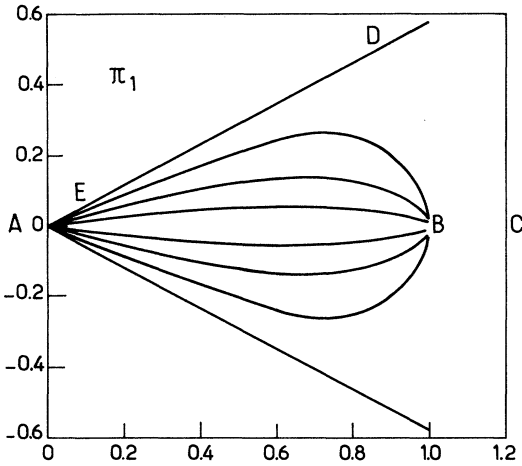


FIG. 1. Self-similar shapes for a divergent flow corresponding to a sector of $\theta_0=60^\circ$. The chosen λ parameters increase from the inner to the outer profile and is equal successively to 0.25, 0.5, and 0.75.

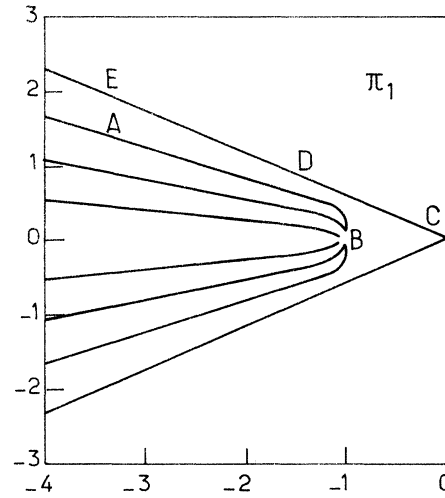


FIG. 2. Self-similar shapes for a convergent flow corresponding to a sector of $\theta_0=-60^\circ$. The chosen λ parameters increase from the inner to the outer profile and is equal successively to 0.25, 0.5, and 0.75.

tor of the π_1 plane is sent to either $-\infty$ (for divergent flow) or $+\infty$ (for convergent flow) in the π plane and the pushing air flux comes from $-\infty$ for the two situations involved here. In the π plane, the velocity potential remains Laplacian, but the continuity relation between the normal velocity at the interface and the potential gradient is modified¹⁶ to

$$\mathbf{n} \cdot \nabla \Phi = \frac{1}{2} |\theta_0| r_1 (\mathbf{n}_1 \cdot \nabla \Phi_1) = \frac{1}{2} \theta_0 A(t) A'(t) \exp(\theta_0 x) \sin(\theta') \quad (1)$$

with $A(t)A'(t) = \pm 1$, $\theta' = \theta + \pi$, $r_1 = (x_1^2 + y_1^2)^{1/2}$, and θ' the angle between the finger-velocity direction at the nose and the tangent at the interface (see Fig. 3). $A(t)$ represents the derivative of the time-evolution function of the interface. In the π plane, half the cell width is chosen as the length unit. As far as possible, we will use the same notations as Ref. 3. The quantity $\frac{1}{2} \theta_0 A'(t) A(t)$, which is always positive, can be related to half the pushing flux Q_0 and plays the same role as U , the finger velocity in the ST experiment. Equation (1) shows a simple proportionality relation between the two normal gradients (up to a stretching factor) which greatly simplifies the following treatment. We are ready now to follow the McLean-Saffman³ (MS) conformal mapping method. The streamline potential Ψ vanishes on the centerline of the π plane and once derivated against the dimensionless arclength S (chosen positive here), is equal to the right-hand side of (1) for each point of the interface. Let us construct an analytical function $H(z)$ that has an imaginary part (here Im) equal to Ψ both on the interface and the centerline. For a point of the interface, we have

$$\text{Im}[H(M)] = \left| \frac{\theta_0}{2} \right| \int_0^S dS \exp(\theta_0 x) \frac{dy}{dS}, \quad \text{with } M = (x, y).$$

Moreover, its value on the wall ED , fixed by the flux conservation, is constant and equal to Q_0/λ with $Q_0 = \text{Im}[H(A)]$, with A located in the tail: $A = (-\infty, \lambda)$.

The conformal mapping transforms the infinite strip potential plane into the upper σ plane: $\sigma = s + it = \exp[-\pi(w - w_0)]$, with w the dimensionless complex potential $w = (\Phi + i\Psi - H)/(1 - \lambda)Q_0/\lambda$ and w_0 as its value at the nose of the finger. In the linear geometry, w is simply the velocity potential in the frame of the moving finger. The interface occupies the segment $0 < s < 1$ on the real axis, the centerline BC the half line $1 < s < \infty$, and the upper wall DE the half line $-\infty < s < 0$. Note that $\theta = 0$ on BC and DE , which is a very useful result for the following. At this stage, the interested reader may think that we can save the first conformal map and go directly from the π_1 plane to the σ plane. It is clear that

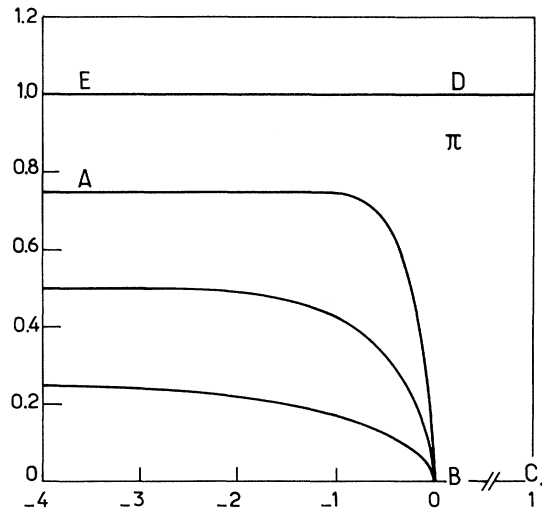


FIG. 3. Self-similar shapes, after conformal mapping, for a divergent flow corresponding to a sector of $\theta_0=60^\circ$. The chosen λ parameters increase from the inner to the outer profile and is equal successively to 0.25, 0.5, and 0.75.

we can pass over directly from π_1 to σ , meaning we can open the half sector from $|\theta_0/2|$ to π . Doing that, we lose the correspondence between both geometries; $\theta_0=0$ and $\theta_0 \neq 0$, which is very useful, since the $\theta_0=0$ instability is now well understood. This possibility must be kept in mind in order to save tedious calculations. As in Ref. 3, we introduce the complex derivative of the potential w , $q \exp(-i\theta)$. We normalize this function by fixing its value to 1 in the tail of the finger ($s=0$) [see Eq. (18) of Ref. 3].

To establish the first equation for the profile, we use the fact that the interface is equipotential and we deduce (Re denotes the real part)

$$\begin{aligned} \frac{\partial \text{Re}(w)}{\partial S} &= \frac{q}{1-\lambda} = -\frac{\lambda}{(1-\lambda)Q_0} \frac{\partial}{\partial S} \text{Re}(H) \\ &= \frac{\pi s q}{1-\lambda} \frac{\lambda}{(1-\lambda)Q_0} \frac{\partial}{\partial s} \text{Re}(H), \end{aligned}$$

since $dS = -ds(1-\lambda)/\pi qs$. The Cauchy integral theorem gives us $\text{Re}(H)$ once the imaginary part of H along the whole s axis is known:

$$\text{Re}(H) = \frac{Q_0}{\lambda \pi} \ln(s) + \frac{1}{\pi} P \int_0^1 dt \frac{\text{Im}H(t)}{t-s},$$

where P is the principal part of the integral. Taking into account the last couple of equations, we get without any difficulty, after some algebra, the following integral equation for the interface:

$$P \int_0^1 dt \frac{\exp(\theta_0 x) \sin(\theta)}{q(t-s)} = \int_0^1 dt \frac{\exp(\theta_0 x) \sin(\theta)}{qt}. \quad (2)$$

Note that for $\theta_0=0$, we must recover the ST solution. This integral equation has a well-known solution, found a long time ago by ST (Ref. 1) and MS (Ref. 3) and the integrand of the left-hand side has the same value as for $\theta_0=0$ up to a proportionality constant that is $a[s/(1-s)]^{1/2}$. It is not necessary to be more precise concerning the constant a of proportionality for the following. Do not forget that x is also a function of s , since

$$z = x + iy = -\frac{1-\lambda}{\pi} \int_s^1 dt \frac{e^{iq}}{qt}. \quad (3)$$

We now face three coupled equations [Eqs. (2) and (3), and Eq. (18) of Ref. 3] for three unknown functions of s : $x(s)$, $q(s)$, and $\theta(s)$. To begin the necessary elimination, let us first eliminate the exponential in Eq. (2) simply by derivation:

$$a \frac{\cos(\theta) \sin(\theta)}{q^2} \frac{(1-s)}{s} + (1-s) \frac{d}{ds} \frac{\sin(\theta)}{q} = \frac{1}{2s} \frac{\sin(\theta)}{q}$$

with $a = \theta_0(1-\lambda)/\pi$. Then take the Hilbert transform of each term of this equation. Remember that θ vanishes when $s \leq 0$ or $s > 1$. We obtain, without difficulty,

$$\begin{aligned} \frac{a}{2} \left[\frac{\cos(2\theta)}{q^2} \frac{1-s}{s} - \frac{1}{s} + \frac{1}{(1-\lambda)^2} \right] + (1-s) \frac{d}{ds} \frac{\cos(\theta)}{q} \\ = \frac{1}{2} \left[\frac{\cos(\theta)}{qs} - \frac{1}{s} \right]. \end{aligned}$$

These two equations are no more than the imaginary and

real parts of the following Riccati equation¹⁷ for the analytical function $G = e^{i\theta}/q - 1$:

$$\begin{aligned} \frac{d}{ds} G &= -\frac{a}{2} \frac{G^2}{s} + G \left[\frac{1}{2s(1-s)} - \frac{a}{s} \right] \\ &\quad - \frac{a}{2} \left[\frac{1}{(1-\lambda)^2} - 1 \right] \frac{1}{(1-s)}. \end{aligned}$$

Note that G must vanish for $s=0$. This nonlinear equation may appear rather complicated to the reader and, at this stage, the improvement rather weak. Nonetheless, it is really an improvement, since we have transformed a free-boundary problem (impossible to solve) into a unique nonlinear differential equation for the interface. A standard substitution transforms a Riccati nonlinear differential equation of the first order into a linear homogeneous differential equation of the second order. Most of the time, there is no closed-form solution to this associated linear equation, but it happens here that it is the standard equation of hypergeometric functions F .¹⁷ The details to derive the solution will not be given here; one only has to follow the method of Ref. 17 without any subtlety and we obtain

$$\begin{aligned} x_1 &= \epsilon(\theta_0) s^{\theta_0(1-\lambda)/2\pi} \\ &\quad \times F \left[\frac{\theta_0(2-\lambda)}{2\pi}, -\frac{\lambda\theta_0}{2\pi}, \frac{1}{2}, 1-s \right], \\ y_1 &= A s^{\theta_0(1-\lambda)/2\pi} (1-s)^{1/2} \\ &\quad \times F \left[\frac{1}{2} + \frac{\theta_0(2-\lambda)}{2\pi}, \frac{1}{2} - \frac{\lambda\theta_0}{2\pi}, \frac{3}{2}, 1-s \right], \end{aligned}$$

with

$$A = 2 \tan \left[\frac{\lambda \epsilon(\theta_0) \theta_0}{2} \right] \frac{\Gamma[1 - \theta_0(2-\lambda)/2\pi] \Gamma(1 + \lambda\theta_0/2\pi)}{\Gamma[\frac{1}{2} - \theta_0(2-\lambda)/2\pi] \Gamma(\frac{1}{2} + \lambda\theta_0/2\pi)}$$

and $\epsilon(\theta_0)$ the sign of θ_0 .

Attempts to simplify the writing of this solution were not successful except for special values of θ_0 : 0, $\pi/2$, $-\pi/2$, and π . In the first case, we recover the ST solution after the necessary mapping $\pi_1 \rightarrow \pi$. The two following cases corresponding to right-angle sectors are given by the set of Ref. 2, providing the correspondence $s = \sin^2(2\alpha)$ and $a = \epsilon(\theta_0)(1-\lambda)/2$ (a has been defined here previously and also in Ref. 2).

For divergent flow, we cannot accept that F diverges for $s=0$, since we have required that G vanishes for this value. Moreover, x_1 and y_1 must be monotonic functions of s , so the hypergeometric functions, mentioned above, must not vanish for $0 < s < 1$. As a consequence, the Γ functions cannot have a negative variable. This imposes a lower bound for λ when θ_0 is greater than $\pi/2$: $\lambda_{\min} = 2 - \pi/\theta_0$ (found in another way in Ref. 16) and an upper bound $\lambda_{\max} = -\pi/\theta_0$ for θ_0 values less than $-\pi$. This means that unique fingerlike solutions of this kind cannot exist for these extreme θ_0 values. For $\theta = \pi$, the only possible solution ($\lambda = 1$) is the half circle.

Finally, the simplest way to illustrate these solutions is to compute a few terms of the Gaussian hypergeometric

series.¹⁷ As an example, I have drawn in Figs. 1 and 2 some typical cases corresponding to $\theta_0 = \pm 60^\circ$. When compared to results of Ref. 2, the convenient profiles superimpose the experimental fingers.² They can also be compared to diffusion-limited aggregation simulations, since it has been shown² that the average of time-dependent patterns are well represented by steady-state fingers at vanishing surface tension. Perhaps these

closed-form solutions will be of some help in understanding the λ -selection mechanism by a small surface tension.⁶ I have found that this formulation in terms of the MS variables is very convenient for a numerical approach, which will be the subject of a separate publication.

I am very grateful to Y. Couder, V. Hakim, M. Rabaud, and S. Tanveer for very instructive discussions.

-
- ¹P. G. Saffman and G. I. Taylor, Proc. R. Soc. London, Ser. A **245**, 312 (1958).
- ²H. Thomé, M. Rabaud, V. Hakim, and Y. Couder, Phys. Fluids A **1**, 224 (1989); A. Arneodo, Y. Couder, G. Grasseau, V. Hakim, and M. Rabaud, Phys. Rev. Lett. **63**, 984 (1989).
- ³J. W. McLean and P. G. Saffman, J. Fluid Mech. **102**, 455 (1981).
- ⁴For a review, see D. A. Kessler, J. Koplik, and H. Levine, Adv. Phys. **37**, 255 (1988); P. Pelcé, in *Perspective in Physics*, edited by H. Araki, A. Libchaber, and G. Parisi (Academic, San Diego, 1988).
- ⁵Y. Pomeau and M. Ben Amar, in *Solids Far from Equilibrium*, edited by C. Godreche, Beg-Rohu Lectures (Cambridge Univ. Press, Cambridge, England, in press).
- ⁶E. A. Brener, D. A. Kessler, H. Levine, and W.-J. Rappel, Europhys. Lett. **13**, 161 (1990).
- ⁷P. G. Saffman, J. Fluid Mech. **173**, 73 (1986); G. M. Homsy, Annu. Rev. Fluid Mech. **19**, 271 (1987); P. Tabeling, G. Zocchi, and A. Libchaber, J. Fluid Mech. **177**, 67 (1987).
- ⁸J. M. Vanden-Broeck, Phys. Fluids **26**, 2033 (1983).
- ⁹D. Bensimon, L. Kadanoff, S. Liang, B. Shraiman, and C. Tang, Rev. Mod. Phys. **58**, 977 (1986).
- ¹⁰B. Shraiman, Phys. Rev. Lett. **56**, 2028 (1986); D. C. Hong and J. Langer, *ibid.* **56**, 2032 (1986); R. Combescot, T. Dombre, V. Hakim, Y. Pomeau, and A. Pumir, *ibid.* **56**, 2036 (1987); S. Tanveer, Phys. Fluids **30**, 1589 (1987).
- ¹¹A. T. Dorsey and O. Martin, Phys. Rev. A **35**, 3989 (1987).
- ¹²Y. Couder, N. Gerard, and M. Rabaud, Phys. Rev. A **34**, 5175 (1987).
- ¹³D. A. Kessler and H. Levine, Phys. Rev. A **32**, 1930 (1985); S. Tanveer, Phys. Fluids **30**, 2318 (1987).
- ¹⁴W.-S. Dai, L. P. Kadanoff, and S. M. Zhou (unpublished); S. Tanveer (unpublished).
- ¹⁵J. Bataille, Rev. Inst. Fr. Pet. **23**, 1349 (1968); L. Paterson, J. Fluid Mech. **113**, 513 (1981).
- ¹⁶M. Ben Amar, V. Hakim, M. Mashaal, and Y. Couder (unpublished).
- ¹⁷C. Bender and S. Orszag, *Advanced Mathematical Methods* (McGraw-Hill, New York, 1978); M. Abramowitz and I. A. Stegun, *Handbook of Mathematical Functions* (Dover, New York, 1980).